SEISMIC EVENT LOCATION STRATEGY AND PATH CALIBRATION IN AND AROUND THE INDIAN SUBCONTINENT

Chandan K. Saikia and Gene Ichinose

URS Group, Inc.

Sponsored by Defense Threat Reduction Agency

DTRA01-00-C-0033 and DSWA01-98-C-0146

ABSTRACT

The primary objective of this study is to obtain reliable earthquake locations ($4<M_W<6$) that occur in and around the Indian subcontinent for reliable calibration parameters for the region. Unlike many other regions of the world, our study region often lacks easy access to local seismic data. Thus, it has become essential to establish a procedure that can be used to improve locations of seismic events that satisfy the ground truth (GT25) criteria. To this end, we find that for an event that satisfies GT10 criteria one can remove all the local and regional phase data within 30^o and can still produce locations comparable to the GT10 results when the depth is independently determined. For moderate sized events, locations become biased due to the poor azimuthal distribution of seismic stations. This influences the trade-off between the depth and the origin time. We have examined our approach by applying to events whose locations were also determined using synthetic aperture radar interferometry (InSAR) analysis. We find that seismic locations determined by our approach remained within 5 km of these locations. Though the InSAR locations may not coincide with the dynamic seismic locations for the larger events because of the size of the fault, they are, however, fairly close for moderate sized events ($M_W \sim 5.5$). We have applied this location approach to identify GT10 events that are within 20^o of NIL in Pakistan, EVN in Nepal, and COC of Sri Lanka. In addition, we have also compiled several catalogues of earthquakes occurring along the northern, central, eastern and western Himalayan Mountain surrounding the Indian subcontinent. We have relocated events from two aftershock sequences, one sequence occurring following the Chamoli earthquake of March 28, 1999, and the other following the Jabalpur earthquake of May 21, 1997. We have also relocated earthquakes occurring in northeast India using the JHD (Joint Hypocenter Determination) technique. International Monitoring System (IMS) stations also record many of these events. We have further identified additional aftershocks that followed India's Republic Day Earthquake of January 2001 (M_W 7.7) which meet the GT10 event location criteria. We are now in the process of yielding an empirical travel-time correction surface for the region using these new GT10 events, including the events from the Koyna region. We have developed regional models for various regions of the Indian subcontinent using travel-time data from the in-country scientific studies and regional waveforms recorded in HYB and regional stations in India.

KEY WORDS:: ground truth, synthetic aperture radar interferometry, IMS, JHD, error ellipse, Rayleigh and Love wave dispersion.

OBJECTIVE

The principal objective of this paper is to present results of our ongoing study on the path calibration for the entire Indian subcontinent to provide model-based P-wave travel times in the region. To accomplish this goal, it is necessary to establish a catalog of earthquakes with quantitative estimates of uncertainties in their ground truth locations. In general, nuclear explosions (when announced) and quarry blasts provide the best ground truth accuracy to within 0 and 2 km. It is, however, difficult to ascertain uncertainties in ground truth locations for earthquakes, especially at low magnitude ($M_W< 4.5$)

The primary objective of this study is to obtain reliable earthquake locations ($4<M_W<6$) that occur in and around the Indian subcontinent for reliable calibration parameters for the region. Unlike many other regions of the world, our study region often lacks easy access to local seismic data. Thus, it has become essential to establish a procedure that can be used to improve locations of seismic events that satisfy the ground truth (GT25) criteria. To this end, we want to demonstrate that for an event that satisfies GT10 criteria, one can remove all the local and regional phase data within 30^o and can produce locations comparable to the GT10 results when the depth is independently determined. In this paper, we will first demonstrate the method and then proceed to apply it to earthquakes occurring in the study region. We will also present results from investigations on regional waveforms that are recorded from earthquakes in northeast India at three stations, namely LSA, CHTO and KMI.

RESEARCH ACCOMPLISHMENTS

Unlike many regions in the world where calibration shots are plentiful with ground truth (GT) accuracy from zero to 2 km, there are only a few such documented events in the study region with precisions that include the nuclear explosions of 1974 and 1998 in India and of 1998 in Pakistan. However, many earthquakes spanning a wide range of magnitude and depth occur along the Himalaya Mountain range from the northwest province in Pakistan to the northeast region in India extending toward the Indo-Myanmar orogeny. Many large earthquakes occurring in this seismic belt satisfy the criteria of GT25 events. These earthquakes are recorded by many stations at teleseismic and upper-mantle distances, and often are recorded by many stations lying nearly along one azimuth. Since access to local catalogs for arrival times from stations located within India is not often available, the number reduces when the criteria for the GT10 events are applied. In order that the GT25 event locations are improved to within the level of accuracy expected for the GT10 events, we successfully examined a method for a possible synergy between the seismic and InSAR (Synthetic Radar Interferometry) locations, using earthquakes for which the InSAR locations are available. In general, the InSAR images correspond to the static deformation across the fault, and for large earthquakes the dynamic event location does not often coincide with the location inferred from the static deformation estimated from the InSAR images. As the magnitude decreases, the static location itself becomes reflective of its dynamic location. In general, the pattern of the co-seismic deformation associated with an earthquake varies with a depth and focal mechanism. The shallower the event, the more likely that it will be observable in its co-seismic deformation in the radar data.

Testing of Location Strategy

Seismic Locations of GT25 Events Relative to Seis+InSAR/GT10 Locations

We examined the event location strategy using both seismic and InSAR data from the May 17, 1993,-Eureka Valley earthquake ($M_W\approx6$). The middle panel in Figure 1 shows a comparison of different seismic locations, namely RELOC, GT10nF, GT25nF, EHB and ISC, estimated using travel times of P and S waves from regional and teleseismic stations. These locations are not far from the corresponding InSAR location ($37.111^oN\pm0.5$km and $117.79^oW\pm0.6$km, Massonnet and Feigl, 1995; Peltzer and Rosen, 1995). The EHB location is from the catalog produced by Engdahl and his associates. The GT10nF and GT25nF are our locations which are equivalent to the GT10 and GT25 locations, but in this case we fixed the event depth determined the P wave seismogram modeling (top panel). RELOC is the location determined using travel-time data from portable and local permanent stations from the Northern California Seismic Network (NCSN) after applying average station corrections. The upper circle to the right of the middle panel gives the distribution of stations, indicating that a large number of the stations that recorded this event lie along the azimuth between 90^o and 180^o. A comparison of all locations suggests that these seismic locations lie within 10 km of the InSAR location.

We applied the same location approach to the 1998 Indian and Pakistani explosions. Fixing their depths at the surface, we relocated the two 1998 explosions using travel-time data. Locations shown in Figure 2 are based on different seismic phases. The GT1 location for the Indian explosion (Barker *et al*., 1999) lies within 5 km of the GT25nF location. For the Pakistani explosion, seismic locations from various sources are beyond 10 km from the GT1 location.

In a recent analysis, Lohman *et al.* (2001) were able to recover the InSAR location for the M_W5.4 Little Skull Mountain earthquake. Their Table 1 gives parameters for the InSAR locations along with the locations found through other strategies involving regional broadband seismograms (Figure 3). We have used this event for another benchmark calculation to investigate whether our approach will find location as good as its corresponding GT10 location. Lohman *et al.* (2001) found several locations, one with the InSAR data alone at 36.743^{o}N and 116.242^{o}W and another with a joint analysis of the seismic and InSAR synergy at 36.747^{o}N and 116.283^{o}W using the standard southern California/or Mojave crustal model. Since the InSAR location does not have the desired resolution, the joint seismic and InSAR location (referred to as Seis+InSAR location) is of a better quality. The GT25nF location is about 4 km from the Seis+InSAR location. We obtained the GT25nF location using the IASP91 crustal model, used no travel-time corrections for the teleseismic stations and did not account for the azimuthal bias. Included in the figure are also the EHB and GT25n and GT10n locations, n referring to the free-depth location, estimated by us. The GT10nF location that was estimated using stations up to 10^o is in proximity to GT25nF location, and both are about 5.5 km from the Seis+InSAR location. Thus, we not only have a good calibration for the locations of the GT25nF events, but also for a GT10nF event location. In the past the accuracy of the GT10 and GT25 locations could not be examined without the InSAR location.

Application to the Earthquakes in India - May 21,1999, Jabalpur and March 28, 1999, Chamoli

Previous studies (Saikia *et al.*, 1999; 2000; Saikia, 2000) have demonstrated that the crustal structure in central India consists of two layers on a half space by successfully modeling regional waveforms recorded at regional stations, namely HYB (Hyderabad), BHPL (Bhopal) and Bilaspur (BLSP), from the May 21, 1997 Jabalpur earthquake. Recently our study was extended to include an investigation of broadband waveforms recorded by regional stations in India from the March 28, 1999, Chamoli earthquake (IMD, Indian Meteorological Department 2000). We found that when seismic waves traverse from northern India through the Gangetic basin, they disperse significantly, and the P_{nl} wave travel times relative to the well-dispersed surface waves, including the dispersion characteristics observed in the surface waves, become path dependent (Saikia *et al.*, 2001). These observations do correlate with the varying thickness of the Gangetic sedimentary basin, further confirmed by the modeling of the recorded waveforms. We relocated these two earthquakes using focal depths determined from the teleseismic modeling of depth phases and using the P and S-wave travel-time data collected from local catalogs. The May 21, 1997, earthquake occurred following the installation of a regional broadband network in India, which generated regional seismograms providing an optimal azimuthal station coverage. Using both P and S travel times from catalog (IMD, 1999), we relocated this event, location shown by REG, using a local crustal model.

Next, we relocated the event by removing all stations within 30^o, essentially making it a GT25 event. The earthquake was recorded by a large number of stations worldwide; many stations reporting travel times for the depth phases also. Figure 4 shows all locations determined for this event, including the corresponding error ellipses where all locations cluster to within 3 km. Since information from sources other than seismic are not available, we can only argue based on the analysis of the Little Skull Mountain (M_W 5.4) and Eureka Valley (M_W 6.0) earthquakes that itsGT25nF location is probably accurate to about 10 km. Following the main event, a temporary network of many stations, shown by triangles in Figure 5, was installed in the epicentral region and recorded about 29 aftershocks (M_L<4), all satisfying the GT10 event location criteria. We relocated these events using the JHD (Joint Hypocenter Determination, Figure 5). Each line connecting a square to a circle represents a shift in relocations relative to the IMD locations. Of these, only the largest event was recorded at teleseimic distances. Figure 6 shows the residuals over the Indian subcontinent relative to our new location and IASP91 crustal model. The March 1999 Chamoli earthquake (M_W 6.7) also generated several aftershocks with M_W > 4. We obtained JHD relocations for these events using travel times from local catalogs and estimated travel-times residuals for P waves at all teleseismic distances (Saikia, *et al.*, 2001).

Path Calibration Study Surrounding Northeast India

Figure 7a shows a variation in travel times for P and S-wave first arrivals as a function of epicentral distances taken from monthly ISC (International Seismological Center) bulletins for $\Delta > 3^{o}$ and from local catalogs for $\Delta < 3^{o}$. The solid lines are least-squares fit with the Pn, Pg, Sn and Sg velocities inverted from the slope of these curves. Figure 7b shows the earthquakes and stations used in this analysis. We relocated these events using JHD method in which we also perturb through the crustal model. Figure 7c shows the travel time curves relative to our new locations which suggest that the average Pn velocity is 7.8 km/sec, lower than 8.33 km/sec that was obtained from the travel-time data before relocations.

Characterization of Surface Waves Using Seismograms at LSA

We collected broadband regional waveforms recorded at LSA from earthquakes (M_W>5.0) occurring within20^{o} of station LSA and analyzed both Rayleigh- and Love-wave dispersion curves using Herrmann's computer package, which uses the multiple-filter technique of Dziewonski. The group-velocity dispersion curves are complex in nature, exhibiting scatters at short periods (<10s), which relates to the complexity of the structure in the region. Figure 8 shows some examples of well-dispersed waves. We inverted both Rayleigh- and Love-wave dispersion curves and obtained a crustal model as shown in Figure 9 (upper panel) along a path from the Indo-Myanmar region to the station LSA (bottom right). Although this inversion has yielded a low-velocity layer at depth, we find that waveforms are not sensitive to any variation in the material properties of this layer. To the right of upper figure are shown the resolving kernels at different periods. Bottom left figure indicates the fit between the observed and simulated dispersion curves from the inverted crustal model for both Love and Rayleigh waves. We are continuing to develop more models in this region along various paths to station LSA based on the surface-wave dispersion analysis. To validate the P- and S-wave model, we forward modeled (computed seismograms) using the new model and checked to insure that synthetics were able to match the body and surface wave amplitudes and arrival times observed at LSA. The source was determined independently using regional long period waves by moment tensor inversion of three or more stations, namely CHTO, KMI and LSA, at long period (Figure 10). In the lower panel to the right is shown the crustal model and to the left is shown the agreement between data and synthetic seismograms along the path toward the station LSA. Note that this path to station LSA from the epicenter has a deep sedimentary river basin inside the province of Assam. In our previous studies, such a model was not available and was difficult to obtain this agreement for the seismograms for which seismic waves traverse through the sedimentary basin of the river.

Other Related Investigation

The Republic Day earthquake (M_W 7.7) in India had drawn wide spread attention throughout the world because of the human causalities including the structural damages even at large epicentral distances (≈250 km). The ground motion in the epicentral region sustained for an extended period of 90s, which is long. Following this devastating earthquake, scientists visited the epicentral region to investigate surfacial features related to the earthquake and brought instruments to record aftershocks and seismograms. These temporary stations recorded several aftershocks (M_W> 4) which satisfy GT10 criteria. We are using them for estimating of travel-time corrections for stations located at upper-mantle and teleseismic distances. We have also analyzed local short-period seismograms from northeast India in conjunction with the broadband seismograms recorded at LSA to investigate Q values of the region (Duarah *et al.*, 2000).

CONCLUSIONS AND RECOMMENDATIONS

Finding accurate ground-truth locations for earthquakes occurring in and around the Indian subcontinent is often difficult because of the poor azimuthal coverage of the region. In addition, there are logistic difficulties in accessing local earthquake catalogs. In this study, we have demonstrated that we can, however, alleviate this problem by focusing on earthquakes that are shallow (h<10 km) and have M_W> 5.5. We find that shallow earthquakes leave imprints in the form of co-seismic deformation of the earth's surface. Analysis of synthetic aperture radar images along the line of sight is a new emerging technique and has proven that co-seismic

deformation estimated from the fringes in the synthetic radar interferometry images when inverted in conjunction with the seismic data can yield highly reliable event location (Lohman *et al.*, 2001). This study has further demonstrated that for large earthquakes that are recorded by many teleseismic stations and have depths determined independently, their locations can also be derived to the accuracy level of the GT10 events, and sometimes even better. To obtain reliable locations using the seismic method alone for events of lower magnitude which will often be recorded by upper-mantle stations rather than by the teleseismic stations, it is needed that for some events we have locations with highest reliability. We recommend the processing of the InSAR images in conjunction with the seismic data for some of selected events in areas where seismic monitoring is most warranted. Once these locations are found, they can form the basis for master events to improve locations of other nearby seismic events.

REFERENCES

Barker, B., M. Clark, P. Davis, M. Fisk, M. Hedlin and others (1998). Monitoring Nuclear tests, Science, V281, 1967-1968.

Duarah, R., S. Baruah, and C. K. Saikia (2000). Depth characteristics of Lg waves and estimation of Q values for northeastern India, AGU abstract, San Francisco meeting.

IMD, India Meteorological Department (1999). Jabalpur earthquake of 22nd May, 1997 and its aftershocks, A consolidated document, Government of India, 70p.

IMD, India Meteorological Department (2000). Chamoli earthquake of March 29, 1999 and its aftershocks - A consolidated document, Government of India, 70p.

Lohman, R. B., M. Simons, and B. Savage (2001). Location and mechanism of the Little Skull Mountain earthquake as constrained by satellite radar interferometry and seismic waveform modeling, J. Geophys. Res., in review.

Massonnet, D. and K. L. Feigl (1995). Satellite radar interferometric map of co-seismic deformation field of M-6,1 Eureka Valley, California earthquake of May 1, 1993, Geo. Phys. Res. Lett., 22, 1541-1544.

Peltzer, G. and P. Rosen (1995), Surface displacement of the May 17, 1993 Eureka Valley, California, Earthquake observed by SAR Interferomtery, Science, V268, 1333-1336.

Saikia, C. K., L. Zhu, B. B. Woods and H. K. Thio (1999). Path calibration and source characterization in and around India, 21st Seismic Research Symposium: Tech. For Monit. CTBT, 243-253.

Saikia, C. K. (2000). A method for path calibration using regional and teleseismic broadband seismograms application to the May 21, 1997 Jabalpur, India earthquake, Current Science, Vol 79, 1301-1315.

Saikia, C. K. (2001). Location and focal mechanism of May 21, 1997 Jabalpur earthquake as constrained by regional travel times and seismic waveform modeling, Bull. Seis. Soc. Am., (manuscript in preparation).

Saikia, C. K., G. Ichinose, S. N. Bhattacharya, J. R. Kayal (2001). Location and mechanism of the March 28, 1999 Chamoli earthquake and modeling of regional seismograms to understand the influence of the Gangetic sediment on regional waveforms, Bull. Seis. Soc. Am., (manuscript in preparation).

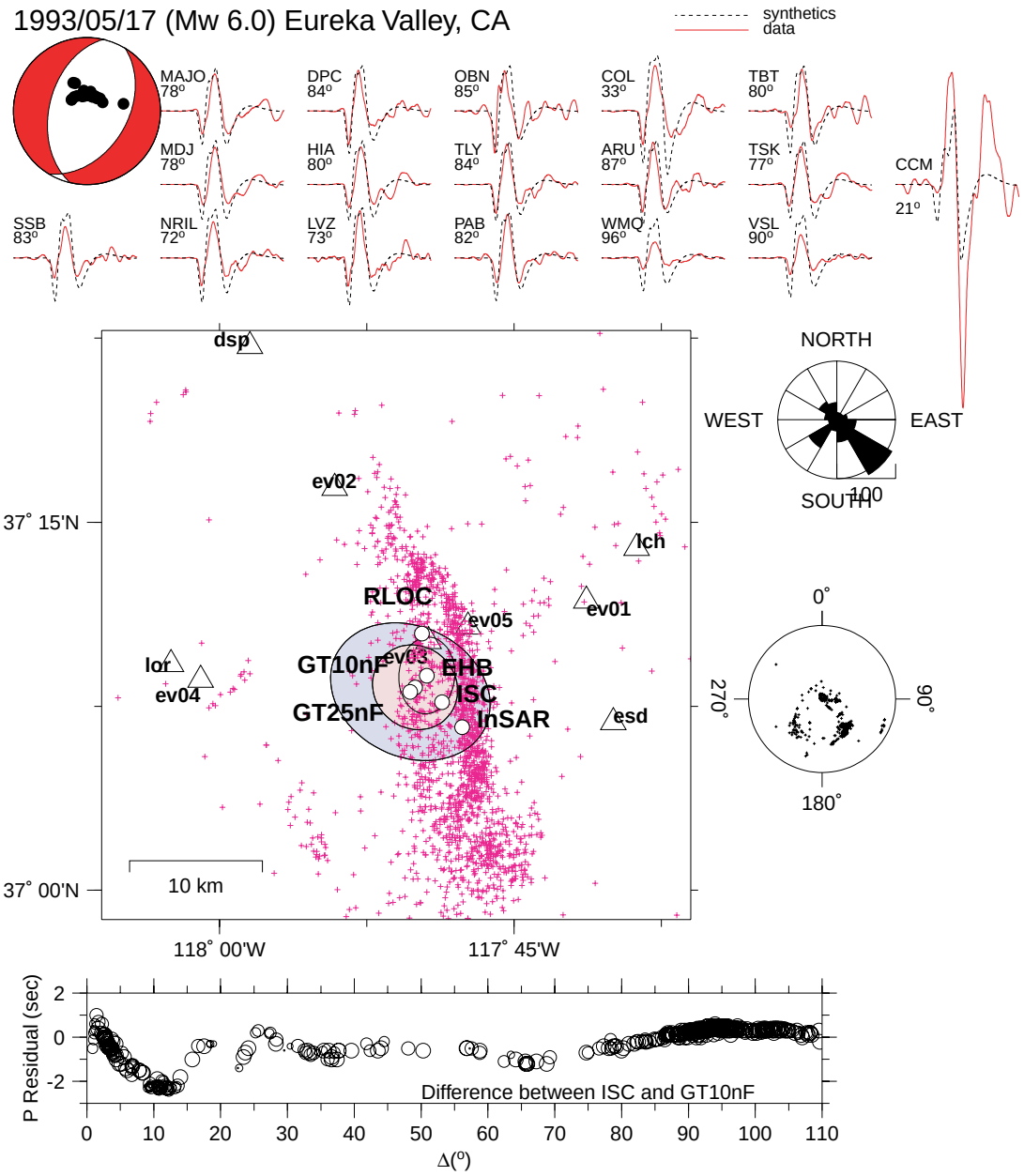

Figure 1. Seismic analysis of the Eureka Valley, California earthquake. (top) Solution and modeled teleseismic P-waves and depth phases (h=14km). The plotted P-waves are shown in velocity, for 42 sec, and at the same amplitude scale. (middle) Location map for portable and permanent seismic stations (triangles) used to relocate the mainshock (RLOC) and over 300 aftershocks (+). Also shown are the GT10nF and GT25nF locations compared to the EHB, ISC, and InSAR locations. The teleseismic station distribution is shown to the right. (bottom) The difference between the ISC and the GT10nF P-wave travel time residuals.

Figure 1. Seismic analysis of the Eureka Valley, California, earthquake (top). Solution and modeled teleseismic P-waves and depth phases (b=14 km). The plotted P-waves are showing in velocity for 42 sec. and at the same amplitude scale (middle). Location map for portable and permanent seismic stations (triangles)used to relocate the mainshock (RLOC) and over 3oo aftershocks (+). Also shown are the GT10nF and GT25nF locations compared to the EHB, ISC, and InSAR locations. The teleseismic station distribution is shown to the right (bottom), The difference between the ISC and the GT10nF P-wave travel-time residuals.

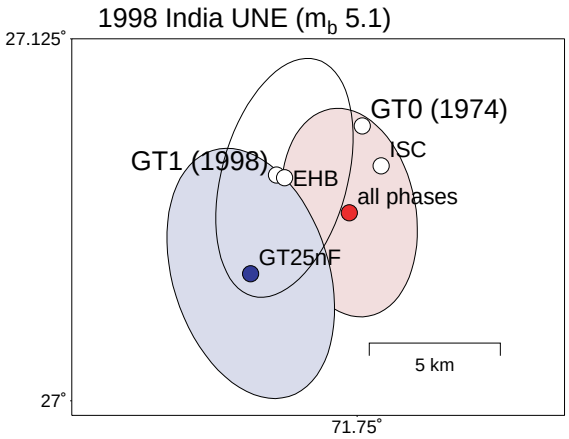

Figure 2a. Location and error ellipses for the 11 May 1998 India nuclear test at the Pokaran test site. The labels "all phases" are given to events which did not fall into the GT10 criteria. The GT25nF location is within 5 km of the GT1.

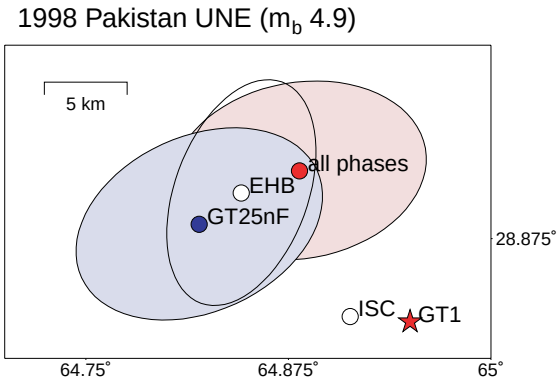

Figure 2b. Location and error ellipses for the 28 May 1998 Pakistan nuclear test. The GT25nF location is within 14 km of the GT1.

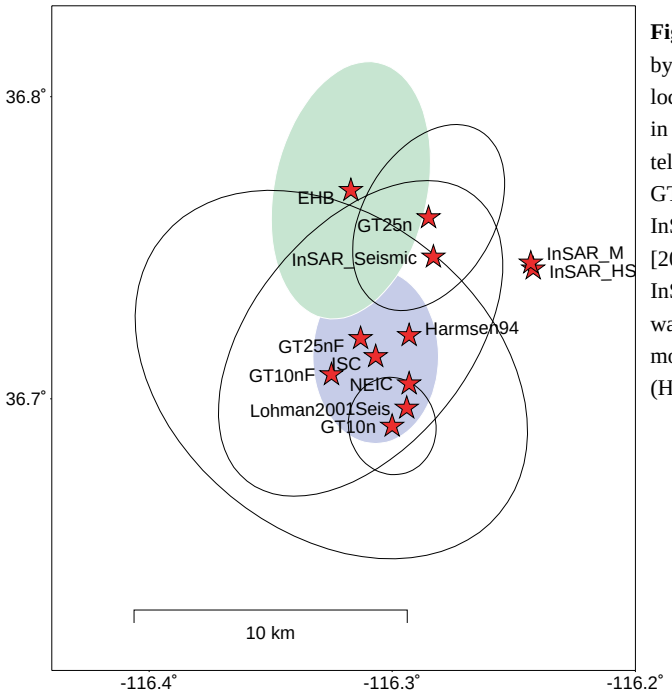

Figure 3. Comparison between locations obtained by seismic and InSAR methods. The GTXnF locations are determined using the criteria described in the text with a fixed depth determined using teleseismic P-waveform inversion results. The GT25nf and GT25n are within 10 km of the joint InSAR and seismic location by Lohman et al. [2000].
InSAR_Seismic location obtained using both seismic waveforms and InSAR with the Southern California model. InSAR_M (Mojave Model), InSAR_HS (Halfspace Model).

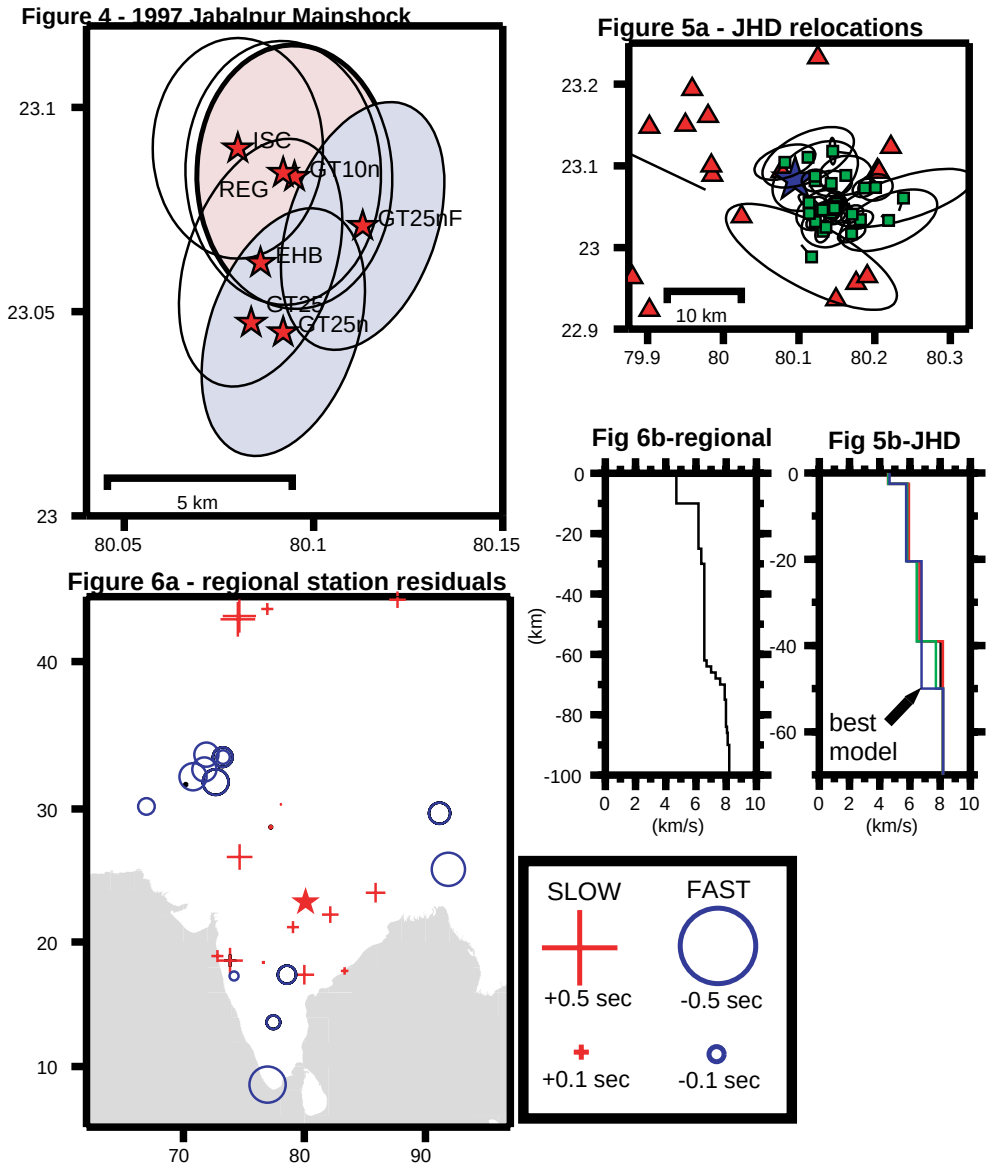

Figure 4. Location map and error ellipses for the 21 May 1997 Jabalpur, India earthquake (Mw 5.8). The REG location is the local IMD location for the mainshock. We relocated the event using free depth (GT10 and GT25n) and fixed depth (GT10nF and GT25nF) criteria. These locate within 5 km of the REG and GT25 (PIDC) locations. The mainshock focal depth, obtained by waveform inversion, was fixed in the relocations [Saikia, 2000]. **Figure 5a** -The aftershock sequence was recored by portable IMD stations and relocated using the JHD method. The relocations are shown as squares and the line points from the IMD location. **Figure 5b** shows the P-wave velocity models obtained from different JHD iterations. **Figure 6a** - The station residuals from the well located Jabalpur mainshock (shown as star) are computed relative to a regional reference P-wave velocity model shown in **Figure 6b.**

Figure 4. Location map and error ellipses for the 21 May 1997 Jahalpur, India, earthquake (Mw 5.8). The REG location is the local IMD location for the mainshock. We relocated the event using free depth (GT10 and GT25) and fixed depth (GT 10nF and GT25nF) criteria. These locate within 5 km of the REG and GT25 (PIDC) locations. The mainshock focal depth, obtained by waveform inversion, was fixed in the relocations (Saikia, 2000). Figure 5a: the aftershock sequence was recovered by portable IMD stations and relocated using the JHD method. The relocations are shown as squares and the line points from the IMD location. Figure 5b shows the P-wave velocity models obtained from different JHD locations. Figure 6a: the station residuals from the well located Jabalpur mainshock (shown as star) are corrupted relative to a regional reference P-wave velocity shown in Figure 6b.

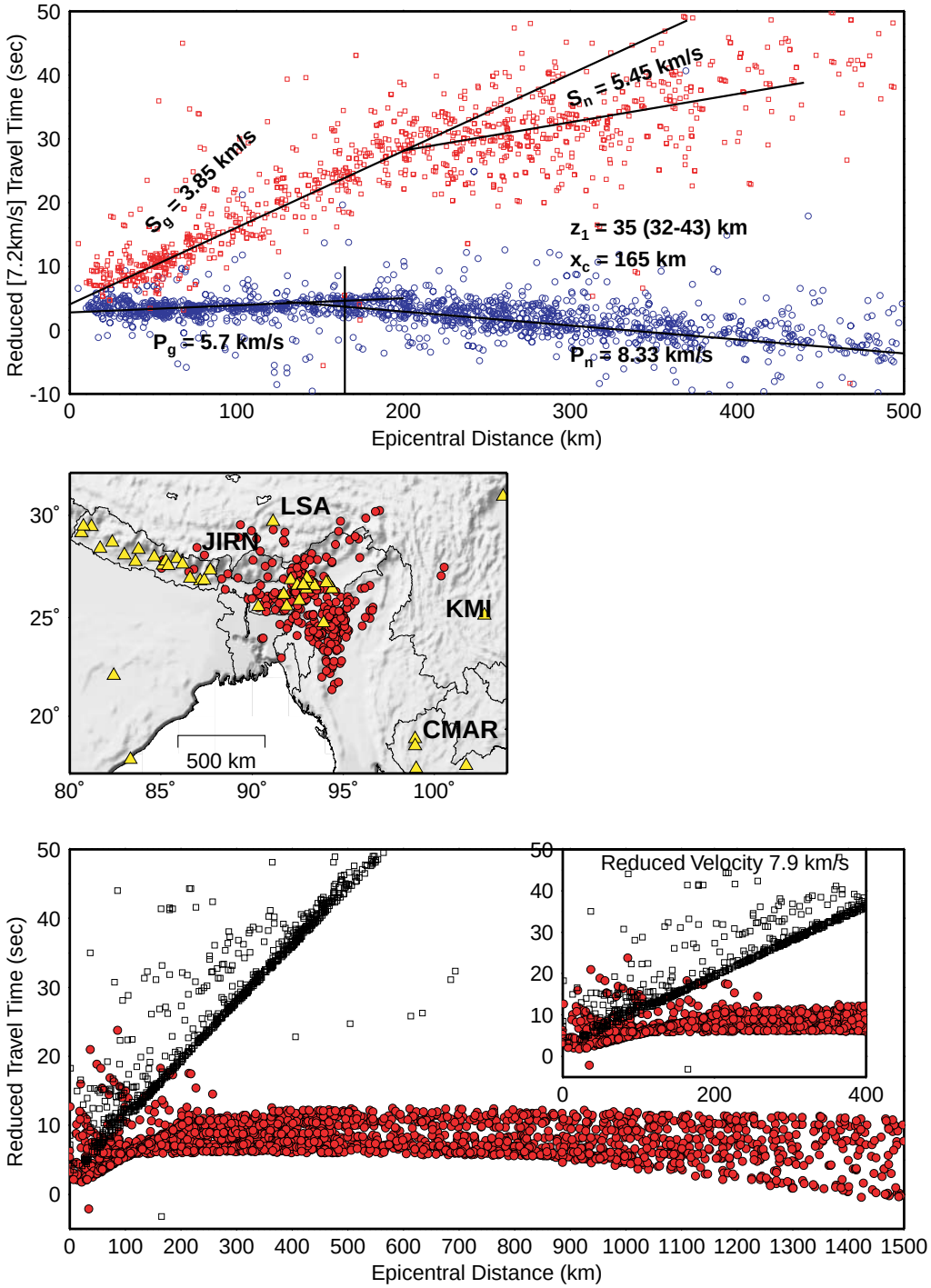

Figure 7. Reduced travel times for north east India earthquakes using phase data from the IMD, NGRI, and stations that report to the ISC. Simple 2-layer interpretations are plotted on the graph. The bottom plot shows the reduced predicted travel times after relocations using station corrections and 1-D model optimization. The times shown are observed travel time plus the residual.

Figure 7. Reduced travel times for northeast India earthquakes using phase data from the IMD NGRI and stations that report to the ISC. Simple two-layer interpretations are plotted on the graph. The bottom plot shows the reduced predicted travel times after relocations using station corrections and 1-D model optimization. The times shown are observed travel-time plus the residual.

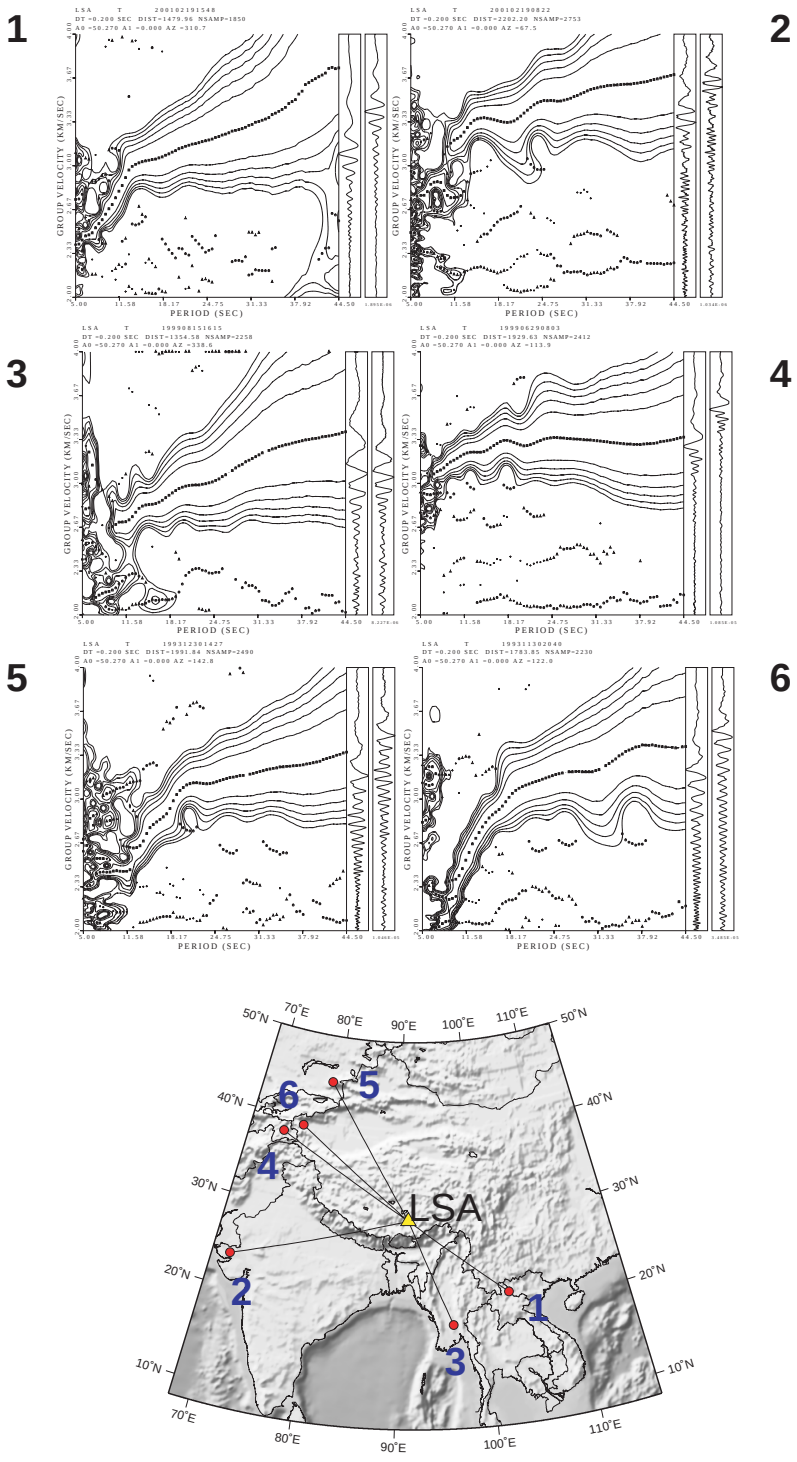

Figure 8. Love-wave dispersion curves for 6 paths from station LSA across southeast Asia.

Figure 8. Love-wave dispersion curves for six paths from station LSA across southeast Asia.

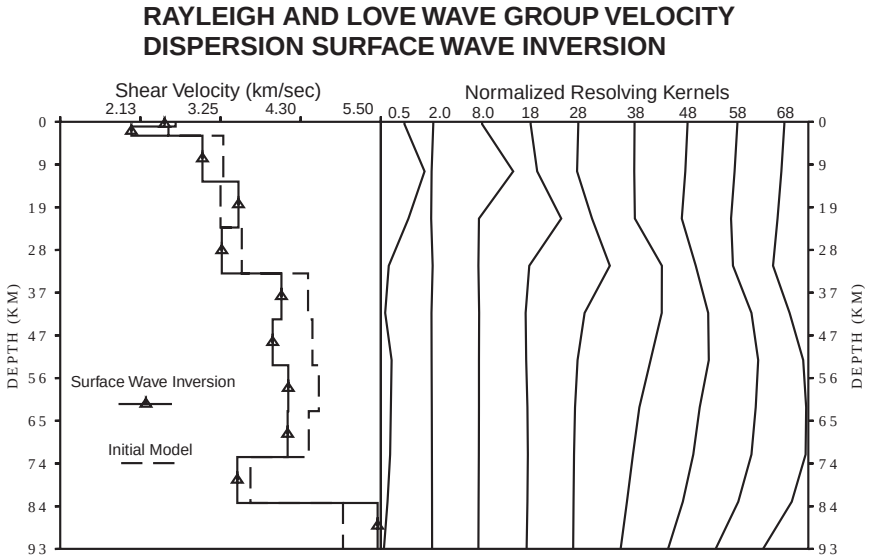

The initial S-wave velocity model was derived from the JHD of P-phase arrivals and Poisson ratio of 0.25. The resolution is best in the middle crust (0 to 28 km) for dispersion measurements between 8 and 28 seconds.

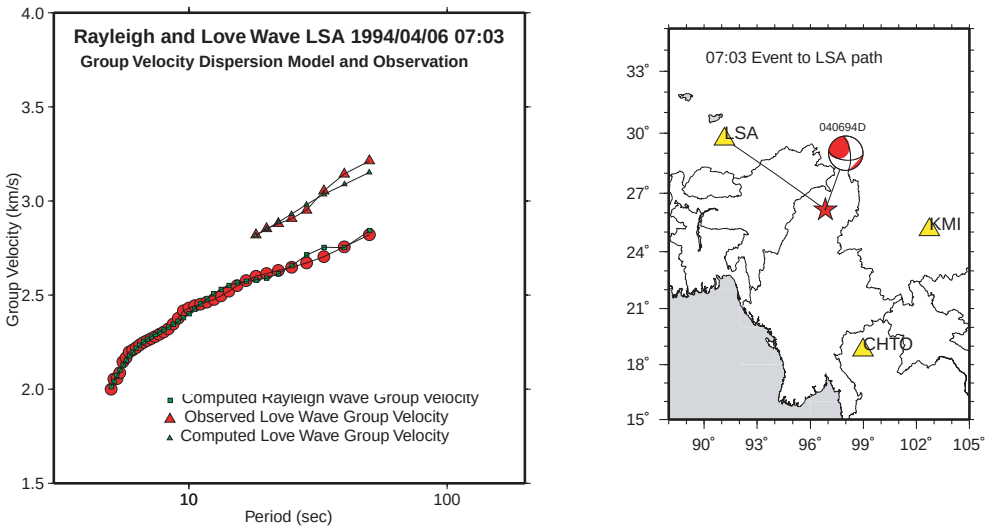

Figure 9. Observed and predicted Love and Rayeigh wave group velocity dispersion curves were inverted for the 1-D S-wave velocity structure for the path between LSA and event 04/06/94 07:03UT.

Figure 9. Observed and predicted Love- and Rayleigh-wave group velocity dispersion curves were inverted for the 1-D S-wave velocity structure for the path between LSA and event 04/06/94 07:03UT.

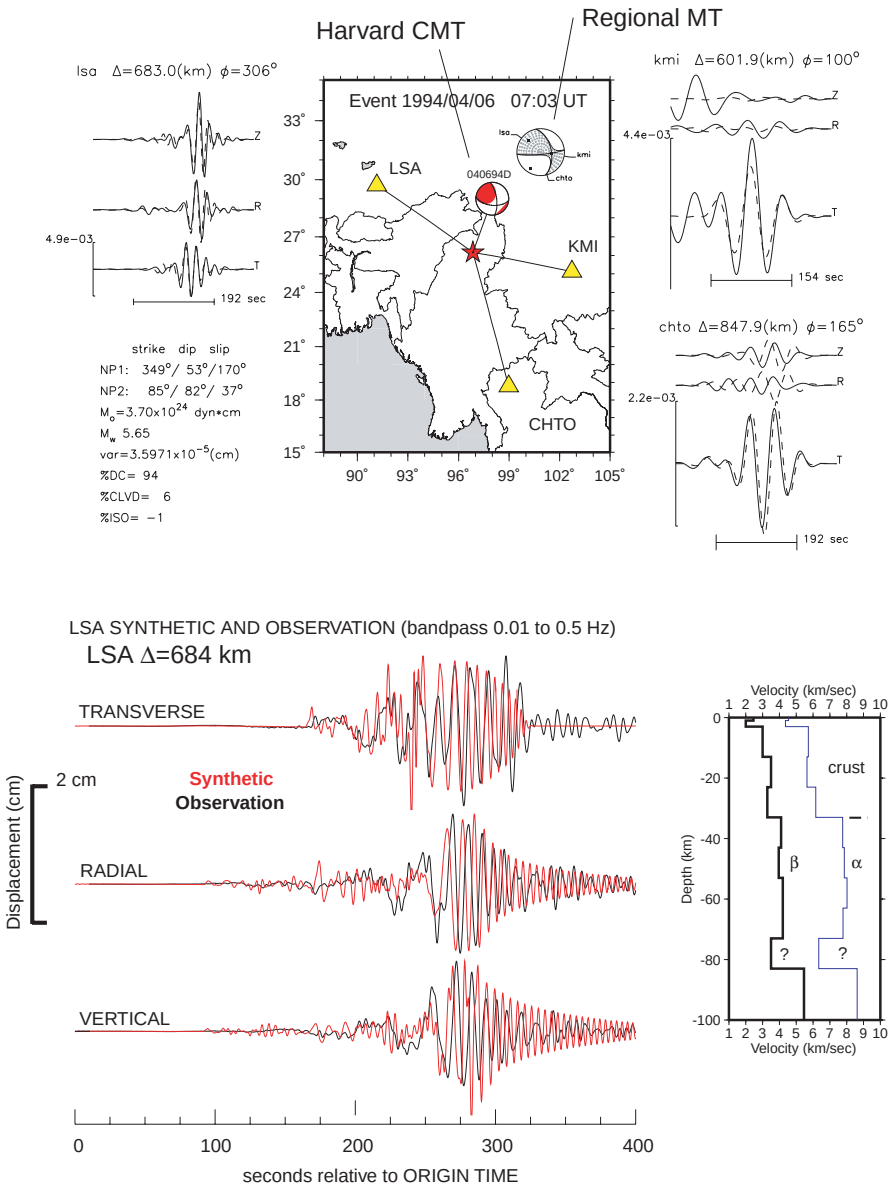

Figure 10. Validation of P- and S-wave velocity model inversion results. We first compute the regional moment tensor solution using long-period waves (50 to 100 sec). The moment tensor is then used to compute synthetic seismograms with the new velocity model. The body and surface waves appear to fit well in the 100 to 2 second period range. The P-wave model is determined using the JHD method on P-phase arrivals. The S-wave model is independently determined by surface wave inversion of group velocity dispersion. The observed waveforms are sensitive to LVZ's in the crust but is not sensitve to the deep LVZ which is not well resoved in the JHD or dispersion analysis.

Figure 10. Validation of P- and S-wave velocity model inversion results. We first compute the regional moment tensor solution using long-period waves (50 to 100 sec). The moment tensor is then used to compute synthetic seismograms with the new velocity model The body and surface waves appear to fit well in the 100- to 2-second period range. The P-wave model is determined using the JHD method on P-phase arrivals. The S-wave model is independently determined by surface wave inversion of group velocity dispersion. The observed waveforms are sensitive to LVZ's in the crust but are not sensitive to the deep LVZ, which is not well resolved in the JHD or dispersion analysis.